Solving three-body-breakup problems with outgoing-flux asymptotic conditions

J. M. Randazzo,[1,*] F. Buezas,[2] A. L. Frapiccini,[1] F. D. Colavecchia,[1] and G. Gasaneo[2]

[1]*División Colisiones Atómicas, Centro Atómico Bariloche and CONICET, 8400 San Carlos de Bariloche, Río Negro, Argentina*

[2]*Departamento de Fĭsica, Universidad Nacional del Sur and CONICET, 8000 Bahĭa Blanca, Buenos Aires, Argentina*

(Received 21 June 2011; published 17 November 2011)

An analytically solvable three-body collision system (s wave) model is used to test two different theoretical methods. The first one is a configuration interaction expansion of the scattering wave function using a basis set of Generalized Sturmian Functions (GSF) with purely outgoing flux (CISF), introduced recently in A. L. Frapicinni, J. M. Randazzo, G. Gasaneo, and F. D. Colavecchia [J. Phys. B: At. Mol. Opt. Phys. **43**, 101001 (2010)]. The second one is a finite element method (FEM) calculation performed with a commercial code. Both methods are employed to analyze different ways of modeling the asymptotic behavior of the wave function in finite computational domains. The asymptotes can be simulated very accurately by choosing hyperspherical or rectangular contours with the FEM software. In contrast, the CISF method can be defined both in an infinite domain or within a confined region in space. We found that the hyperspherical (rectangular) FEM calculation and the infinite domain (confined) CISF evaluation are equivalent. Finally, we apply these models to the Temkin-Poet approach of hydrogen ionization.

DOI: 10.1103/PhysRevA.84.052715 PACS number(s): 34.80.Dp, 31.15.−p, 34.10.+x

I. INTRODUCTION

The three-body breakup problem is of fundamental interest in atomic collisions theory. The simplest example, ionization of atomic hydrogen by electron impact, is theoretically described by the solution of the Schrödinger equation associated with two electrons moving in the field of a heavy nuclei considered at rest. Analytical solutions are not known. However, cross sections for various energies have been measured in the laboratory for this process.

The main theoretical difficulties of the three-body fragmentation problems with Coulomb interactions are related to the very complicated form of the six-dimensional (correlated) wave function together with its asymptotic properties [1–5]. Many separable and nonseparable models have been introduced to obtain approximate values for the transition amplitudes [6,7], which are solutions of the Schrödinger equation in some asymptotic region where at least one of the particles is far away from the other two. However, the applicability of these models is limited: they are not exact solutions of the Schrödinger equation in the whole space [4,5] and only give approximate transition amplitudes.

When a partial wave expansion of the wave function is performed, the problem reduces to a coupled set of two-dimensional equations. Although a partial-wave expansion of the asymptotic form of the exact collisional state has been given [8], its analytical expression is too complicated to benefit numerical calculations. Numerical methods must be able to correctly describe the inner as well as the asymptotic behavior of the wave function, since any incorrect condition would ruin it in the whole space domain, due to the nonlocality of quantum systems.

Aside from these subtleties, numerical procedures are able to obtain accurate cross sections that agree with experimental data. Perhaps one of the most straightforward approaches has been the use of numerical grid methods in the two-dimensional radial domain to solve the Schrödinger equation [9]. The exterior complex scaling (ECS) method [11,12] is very efficient at imposing the adequate asymptotic collisional behavior to the scattering wave function, through rotation of the coordinates to the complex plane. Outgoing flux is related to an exponentially dumped behavior in the rotated coordinates, which is simulated with box boundary conditions in a large square domain. Although outgoing flux in both electron coordinates is related to the double continuum channels, the obtained wave function is valid in the whole spatial domain where overlapping with other channels occurs, since it is the "predominant" behavior when fragmentation take place. Accurate scattering wave functions and breakup cross sections are obtained with the ECS method, although at the price of employing very large numerical grids, which results in huge matrix computational manipulations [13]. Besides, within the framework of this method, an artificial cutoff in some of the interactions is required to make it work.

Other theories such as the J-matrix approach employ spectral techniques to deal with the three-body problem [14,15]. Another method is the convergent close coupling (CCC) [16,17], which is based on the use of one Coulomb function to represent one of the electrons and pseudostates to describe the other one. The method in this form simplifies the coupled two-dimensional radial equations. Pseudostates can be chosen in such a way that they remove the one-electron kinetic energy and the electron-nucleus interaction from the Schrödinger equation. Because pseudostates are used, breakup is evaluated as an excitation process with an appropriate renormalization procedure connected with the one-electron continuum quadrature. This CCC method has been proven to be convergent but, since the expansions are performed in only one of the coordinates, the method cannot be formally considered exact. In most successful applications, a linear set of equations for the (discretized) transition amplitudes is obtained instead of the wave function itself. However, the pseudocontinuum states do not have the correct outgoing-electron asymptotic behavior of the ionizing states. These approximations lead to unphysical oscillations when differential cross-section amplitudes are evaluated, which are also related to the application of two-body formalisms to three-body problems [18,19].

*randazzo@cab.cnea.gov.ar

All these methods consume lots of computational resources, which is the reason why they are continuously tested and improved.

We have recently introduced a family of two-particle Sturmian functions which allows the fulfillment of arbitrary asymptotic boundary conditions in the radial coordinates of the electrons [20,21]. The radial Sturmian functions are evaluated numerically with fast and accurate routines, so a great variety of potentials can be included in the radial equation to perform convergence experiments [22,23]. Using GSF with stationary-wave asymptotic conditions, we were able to calculate very accurate H^- and He bound state energies. They also were used [24] in s-wave fragmentation models by imposing to the basis purely outgoing flux. The solutions where compared with analytical models and previous ECS calculations, showing a higher computational performance of the GSF method over the ECS method. They also were applied to the Temkin-Poet model of hydrogen ionization by electron impact, confirming the applicability of the GSF basis to long-range potential scattering problems.

The technical details of our method for continuum expansions, however, were not presented. The purpose of this work is to analyze deeply the success of the GSF basis with the break up asymptotic conditions. For that purpose, we review the solutions of the previously studied analytically solvable fragmentation s-wave model, which has a highly correlated continuum asymptotic behavior. The problem is solved with a Sturmian expansion and its solution compared with the exact one, and with the solution obtained by a finite element method (FEM). Two kinds of CISF calculations will be performed, which are based on two different definitions of the spatial domain of the wave function: one leads to a wave function in a box domain characterized by the range where the Sturmian generating potential has nonzero value, while the other one is determined in an infinite domain. As we will see, these definitions make a difference in the CI calculations only on the values of the overlap matrices and potential matrix elements when the Galerkin method is applied.

Another aim of this work is to evaluate the impact of the asymptotic condition as a boundary condition with different domain shapes in the calculation of cross sections and their convergence rates. The FEM always evaluates the wave function in a finite two-dimensional radial domain, which can be chosen to have different shapes. One of the FEM calculations is obtained with a circular arc contour where a hyperspherical outgoing flux is imposed exactly. The other domain simulates a box in which outgoing flux is set in its sides.

The results presented here shed some light on the question of how the exact boundary condition is constructed even when different contours are used to solve the problem, both with the use of basis sets or FEM approaches.

The organization of the paper is as follows. In Sec. II we present the two-body Sturmian theory for arbitrary asymptotic conditions. In Sec. III we derive the emission model formulas and their analytical solutions and propose both the Sturmian expansion and FEM solutions for the two different domains. Results are showed in Sec. IV, where the Temkin-Poet $(e,2e)$ problem is studied. Finally (Sec. V), some conclusions are draw.

We employ atomic units ($m = \hbar = e = 1$) throughout.

II. TWO-BODY STURMIAN FUNCTIONS

A. Theory

In this section we briefly review the theory of Weinberg states for positive energies. We present the theory for s-wave models and consider only spherically symmetric potentials [25,26]. Generalization to higher angular momenta is straightforward [20].

Consider the s-wave function for a unitary mass particle in a central spherically symmetric potential. We consider the following Schrödinger equation for the radial function $S_n(r)$:

$$\left[-\frac{1}{2}\frac{d^2}{dr^2} + U_0(r) - E\right] S_n^+(r) = -\beta_n^+ V(r) S_n^+(r), \quad (1)$$

where the potential $V(r)$ is assumed to vanish in an external region $r > r_c$, where $U_0(r)$ or, if not zero, is purely Coulombic: $U_0(r) = Z/r$ for $r > r_c$. This potential V plays an important role in our discussion, and it will be referenced as the *generating potential*. We assume that the function S_n^+ satisfies physical boundary conditions:

$$\lim_{r\to 0} r S_n^+(r) = 0 \quad (2)$$

and

$$\lim_{r\to\infty} r S_n^+(r) \simeq H^+(r), \quad (3)$$

where $H^+(r)$ is the outgoing-flux Coulomb (free when $Z = 0$) wave function:

$$H^+(r) = (-i)e^{\frac{1}{2}\pi\frac{Z}{k}} e^{ikr}(2kr)U\left(1 + i\frac{Z}{k}, 2, -2ikr\right), \quad (4)$$

where $U[a,b,z]$ is the Tricomi hypergeometric function [27].

$H^+(r)$ and has the following eikonal behavior:

$$H^+(r) \to \exp\left\{i\left[kr - \frac{Z}{k}\ln(2kr)\right]\right\} \quad (k = \sqrt{2E}). \quad (5)$$

The function $H^+(r)$ is a positive energy (continuum) solution of Eq. (1) for $r > r_c$ (i.e., $V(r) = 0$ and $U_0(r) = \frac{Z}{r}$), where it reduces to

$$\left[-\frac{1}{2}\frac{d^2}{dr^2} + \frac{Z}{r} - E\right] S_n^+(r) = 0 \quad \text{for} \quad r > r_c. \quad (6)$$

The Sturmian solutions of Eq. (1) and conditions (2) and (3) result by taking the energy E as a fixed parameter and β as the eigenvalue to be determined. The boundary condition (2) ensures the regularity of the wave function at the origin of coordinates, where the potentials V and U_0 might be divergent. By setting Z, $E \in \mathbb{R}$, and $E > 0$ the solution is a nondivergent wave function in the region $r \to \infty$, for any value of β on the complex plane (not true if V is long range [20]). Other asymptotic conditions can be imposed, such as incoming-wave, stationary-wave, and spherical box boundary conditions or any admixture obtained by fixing the value of the logarithmic derivative of S_n at r_c [21]. For the present calculations the spectra of the eigenvalue β are discrete and their values are complex [20,21,28]. Since condition (3) does not depend on the radial quantum number n (except maybe in some overall normalization factor), the set of functions

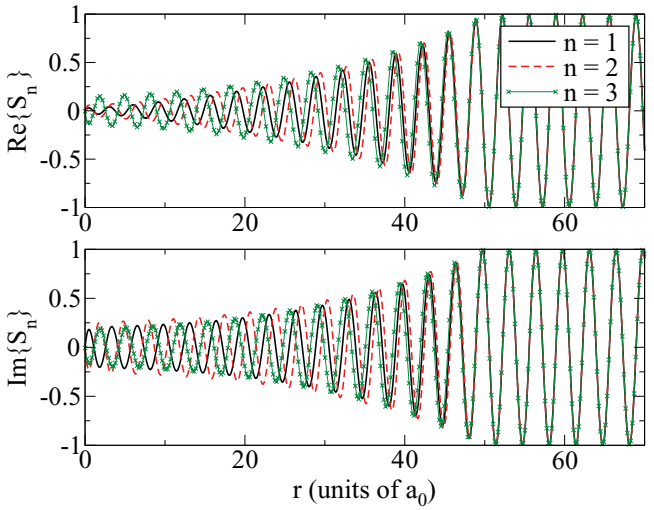

FIG. 1. (Color online) Typical $S^+_{0,n}$ $(n = 1, \ldots, 4)$ solutions of Eq. (1).

$S_n(r)$ have all the same asymptotic behavior (see Fig. 1), corresponding to a particle of energy E outgoing from the nucleus and affected by the Coulomb interaction characterized by the charge Z.

The existence of flux solutions which are regular in the whole space is connected to the complex emissive *short-range* potential $\beta_n V$ in the inner region, $r < r_c$. This can be easily seen if one considers a complex charge in the asymptotic expression of Eq. (5), which would be potentially divergent.

An alternative way to write Eq. (1) is

$$-\frac{1}{\beta_n^+} S_n^+(r) = G^+(r,r')V(r)S_n^+(r), \tag{7}$$

where $G^+(E,r,r')$ is the Green's function associated with the Hamiltonian appearing in the left-hand side of Eq. (1). Clearly, the Sturmians $S_n^+(r)$ are eigenfunctions of G^+V with eigenvalue $-1/\beta_n^+$ and that is why they possess outgoing/incoming behavior at large distances and are appropriate to deal with collision problems [29].

The eigenfunctions S_n defined by Eqs. (1), (2), and (3) satisfy potential-weighted orthonormality conditions of the form

$$\langle S_{n'} | \, V \, | S_n \rangle = \int_0^\infty dr S_{n'}^+(r)V(r)S_n^+(r) = \delta_{n',n}, \tag{8}$$

and the closure relation associated with them can be written as

$$\sum_{n=0}^{\infty} S_n^+(r')S_n^+(r)V(r) = \delta(r - r'). \tag{9}$$

Note that the scalar product and closure relation is defined with the wave function on the left and not by its conjugate [30].

B. Numerical evaluation of the radial equation

There exists a small number of potentials for which analytical solutions of Eq. (1) are known [31,32]. In most of the cases it is possible only to find a solution for $l = 0$. For general potentials, it is necessary to implement a numerical method to obtain S_n^+.

The numerical procedure employed to evaluate the Sturmian functions and eigenvalues for arbitrary potentials and asymptotic conditions has been described in earlier publications [21–23] and will not be presented here. Although the numerical solution of a one-dimensional equation such as Eq. (1) could be simple, it has to be noted that the complex condition (3) produces a non-Hermitian eigenvalue problem, so special care must be taken with the numerical procedures. We recall that the numerical relative precision of the expansion is of the order of 10^{-8}–10^{-9}, small enough for the present purposes.

III. TWO-PARTICLE EMISSION MODEL

Here we study the case of a simple three-particle continuum, such as the s-wave emission of two particles from a correlated source located in the foregoings of the nuclei. We choose this simple model because its exact analytical solution can be easily evaluated and also allows us to compare with ECS calculations [33]. We consider spin-1/2 particles to make the same symmetry considerations as for the electrons.

The scattering wave function for this model satisfies the following Schrödinger equation:

$$\left[-\frac{1}{2}\frac{\partial^2}{\partial r_1^2} - \frac{1}{2}\frac{\partial^2}{\partial r_1^2} - E\right] \Psi_{\rm sc}^+(r_1,r_2) = e^{-r_1-r_2}, \tag{10}$$

together with the regularity condition,

$$\Psi_{\rm sc}^+(r_1,r_2) = 0 \quad \text{for} \quad r_i = 0 \;\; (i = 1,2), \tag{11}$$

and particle-emission asymptotic behavior,

$$\Psi_{\rm sc}^+(r_1,r_2) = -\frac{1}{\sqrt{2}}\left(\frac{iK^3}{\rho}\right)^{1/2} f(\alpha)e^{iK\rho}, \tag{12}$$

where $K = \sqrt{2E}$, $\rho = \sqrt{r_1^2 + r_2^2}$, $\tan\alpha = r_1/r_2$, and $f(\alpha)$ is the dispersion amplitude. Note that for values of r_1 and r_2 such that the driven term $e^{-r_1-r_2}$ is zero, Eq. (10) also admits the asymptotic solution

$$\Psi_{\rm sc}^+(r_1,r_2) = A(e^{ik_1r_1+ik_2r_2} + 1 \longleftrightarrow 2), \tag{13}$$

where $k_1^2 + k_2^2 = 2E$, and $1 \longleftrightarrow 2$ represents the proper symmetrization of the first term: $r_1 \longleftrightarrow r_2$. This is not the standard asymptotic scattering solution, but one which is separable and mathematically admissible for this problem. The spin symmetry of the scattering wave function is given by the symmetry of the right-hand side of the Schrödinger equation. The singlet (triplet) wave function has an even (odd) behavior as a function of α around $\pi/4$. In the present calculations we only consider the singlet component ($S = 0$) for simplicity.

While boundary condition (11) is straightforward, Eq. (12) is much more complicated from the computational point of view, since it has to be imposed on the asymptotic region. In addition, it depends on the breakup amplitude f, which is the fundamental unknown of the problem. When dealing with numerical calculations, asymptotic conditions have to be modeled as a boundary condition. In addition, Eq. (12) is not separable in the radial coordinates of the electrons, which are useful to represent the unperturbed initial states of the

collision. It is a highly correlated state, even when the particles are far from the interaction region. The only advantage of the asymptotic behavior of Eq. (12) is that it is separable in the hyperspherical coordinates (ρ,α) [34]. As we will see, the flux behavior can be imposed as a condition on the logarithmic derivative, without making reference to the breakup amplitude.

We can solve Eq. (12) for the amplitude $f(\alpha)$ in terms of the scattering wave function,

$$f(\alpha) = \lim_{\rho\to\infty} -\frac{\sqrt{2}}{2}\left(\frac{iK^3}{\rho^5}\right)^{-1/2} \Psi^+_{\rm sc}(r_1,r_2)e^{-iK\rho}, \quad (14)$$

from which the single differential cross section can be evaluated:

$$\sigma(\varepsilon) = \frac{1}{k_1k_2}|f(\alpha)|^2. \quad (15)$$

We show in the next two sections that the solution of Eq. (10) with the conditions (11) and (12) can be accurately found using generalized Sturmian Functions (GSFs) as well as with the FEM methods, in a similar way as done by the ECS.

A. The Sturmian expansion

We propose an expansion of the scattering wave function $\Psi_{\rm sc}$ in terms of products of Sturmian functions with outgoing-wave boundary conditions:

$$\Psi^+_{\rm sc}(r_1,r_2) = \sum_{\nu}^{N_b} \varphi_\nu \frac{1}{\sqrt{2}}\left[S^+_{n_1}(r_1)S^+_{n_2}(r_2) + 1 \longleftrightarrow 2\right], \quad (16)$$

where the functions $S^+_{n_i}$ are solutions of Eq. (1) with $E_1 = E_2$ and $U_0 = 0$. The symbol ν stands for the quantum numbers n_1 and n_2, and the sum in the n_1 index of Eq. (16) runs from 1 to the two-body basis size N_s, while n_2 starts running from $n_0 = n_1$ up to N_s. This avoids redundancies in the expansion, due to the fact that only half of the radial domain has to be expanded because of the spin symmetry. The number of three-body basis elements because of this restriction is $N_b = \frac{1}{2}N_s(1+N_s)$.

Replacement of expansion (16) into Eq. (10) gives ($S = 0$)

$$\sum_{\nu}^{N_b} \frac{\varphi_\nu}{\sqrt{2}}\left[\left(-\beta^+_{n_1}V_1 - \beta^+_{n_2}V_2 - \tilde{E}\right)S^+_{n_1}S^+_{n_2} + (1\longleftrightarrow 2)\right] = e^{-r_1-r_2}, \quad (17)$$

where $\tilde{E} = E - E_1 - E_2$. One can see that see that the kinetic energy operator is totally removed from Eq. (10). The short-range generating potentials are present as well as part of the total energy depending on the parametric values of E_1 and E_2. Projecting from the left with all the basis elements (Galerkin method), we end up with the $N_b \times N_b$ system of linear equations for the coefficients φ_ν:

$$[\tilde{\mathbf{V}}_d + \tilde{\mathbf{V}}_e]\boldsymbol{\varphi} = \boldsymbol{\varphi}_0, \quad (18)$$

where

$$\begin{aligned}[\tilde{\mathbf{V}}_d]_{\nu',\nu} &= -\beta^+_{n_1}\langle S^+_{n'_1}|V_1|S^+_{n_1}\rangle\langle S^+_{n'_2}|S^+_{n_2}\rangle \\ &\quad -\beta^+_{n_2}\langle S^+_{n'_1}|S^+_{n_1}\rangle\langle S^+_{n'_2}|V_2|S^+_{n_2}\rangle, \\ [\tilde{\mathbf{V}}_e]_{\nu',\nu} &= -\beta^+_{n_1}\langle S^+_{n'_2}|V_1|S^+_{n_1}\rangle\langle S^+_{n'_1}|S^+_{n_2}\rangle \\ &\quad -\beta^+_{n_2}\langle S^+_{n'_2}|S^+_{n_1}\rangle\langle S^+_{n'_1}|V_2|S^+_{n_2}\rangle,\end{aligned}$$

and

$$[\boldsymbol{\varphi}_0]_{\nu'} = \frac{1}{\sqrt{2}}\left[\langle S^+_{n'_1}|e^{-r}\rangle\langle S^+_{n'_2}|e^{-r}\rangle + (1\longleftrightarrow 2)\right].$$

Some of the one-dimensional integrals of the matrix elements of Eq. (18) are weighted by the generating potentials or decay exponentially. The integration region is limited to $r < r_c$ (where r_c is chosen such that e^{-r_c} is extremely small) and performed with a Gauss-Legendre quadrature. The same strategy is applied for the overlap integrals $\langle S^+_{n'_i}|S^+_{n_i}\rangle$ $(i = 1,2)$ in the range $0 < r < r_c$. However, the Sturmian functions are defined in all space. If we do not take into account the external part of the overlap integrals the evaluation can be interpreted as a box-based-type calculation. The complete (continuum) calculation is performed by using the asymptotic forms of the GSF. By normalizing the GSF to exactly behave as Eq. (5) we get, for the matrix element of any operator W,

$$\begin{aligned}\langle S^+_{n'_1}|W|S^+_{n_1}\rangle &= \int_0^{r_c} S^+_{n'_1}(r)W(r)S^+_{n_1}(r)dr \\ &\quad + \lim_{\varepsilon\to 0}\int_{r_c}^{\infty} dr e^{ik'_1r}We^{ik_1r}e^{-\varepsilon r}. \quad (19)\end{aligned}$$

For example, for the overlap matrix elements present in $\tilde{\mathbf{V}}$ we have $W = 1$ and the second term of the right-hand side of Eq. (19) reads

$$\lim_{\varepsilon\to 0}\int_{r_c}^{\infty} dr e^{ir(k_1+k_2)-\varepsilon r} = \frac{ie^{ir_c(k_1+k_2)}}{k_1+k_2}, \quad (20)$$

where $k_i = \sqrt{2E_i}$ $(i = 1,2)$. Note that the Sturmian functions proposed here are *quasi*-square-integrable, since their scalar product is formally defined for complex values of the momenta, and it is the limit procedure (which is mathematically well defined) which makes the integration possible. In the numerical calculation $\varepsilon/2$ is taken as 0 in the inner region and the expression of the right-hand side of Eq. (19) is used for the exterior part. The two (the complete and the box-based) definitions of the overlap matrix are used in the next section in order to study differences of their results. Generalization of Eq. (20) to the case of outgoing waves with Coulomb logarithmic phases is straightforward.

A direct consequence of using a short-range generating potential V is that all two-body Sturmian functions have the same behavior in the region $r > r_c$. This means that the three-body expansion matches a separable product of outgoing spherical waves in the region $\rho > r_c$, of (externally fixed) energies E_i $(i = 1,2)$. However, correlation and the driven term of Eq. (10) produce a mixing of all continuum (energetically allowed) outgoing channels, whose amplitude is the unknown of the problem. The Sturmian expansion is accurate in the region where such mixing can be expanded, i.e., $0 < r_i < r_c$ $(i = 1,2)$. In the external regions it matches smoothly a wave function with a definite momenta of one or both electrons (depending the region). Although it is not the true asymptotic behavior, we will see that by choosing adequate values of E_i $(i = 1,2)$ and a proper continuum definition of the overlaps [given by Eq. (20)] the outgoing flux is perfectly modeled in the box of size r_c and no numerical reflection problems arises. The accuracy of the expansion is

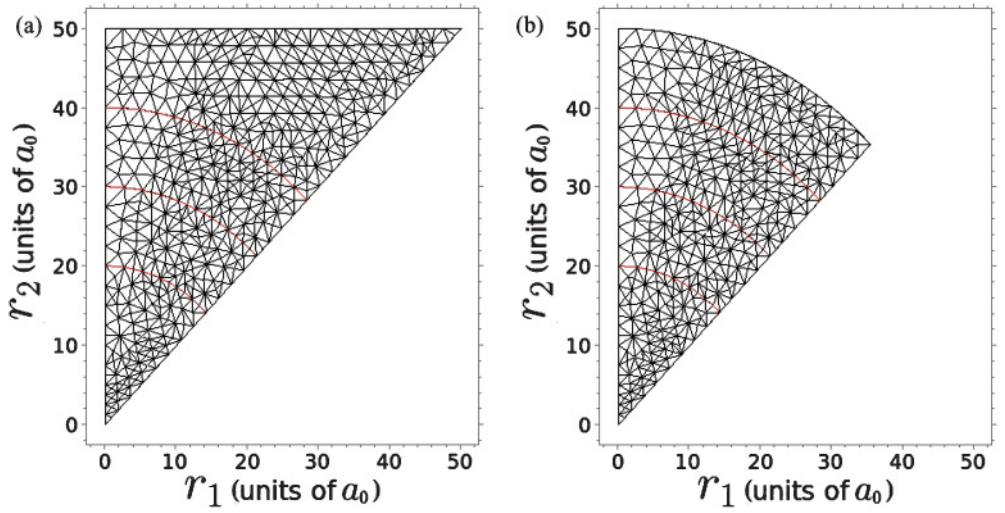

FIG. 2. (Color online) Example of different computational FEM domains and their respective automatically generated mesh.

associated with the density of states in the region expanded by the generating potential V.

Once the matrix elements have been calculated, Eq. (18) can be solved with the ZGESV subroutine of the LAPACK package [35].

B. FEM approximation to scattering problems

An alternative approximation to the scattering wave function can be obtained by solving Eq. (10) directly by means of the FEM calculation, which is not a spectral expansion like the CISF expansion. In this work we present solutions evaluated with the software FLEXPDE [36]. We choose this code because it allows the use of almost arbitrary geometry for the contours of the (r_1,r_2) domain, and it allows one to impose any kind of boundary conditions over them. We consider two domains for Eq. (10): a triangular domain [domain (a), Fig. 2(a)] and a circular sector, closed by two segments [domain (b), Fig. 2(b)].

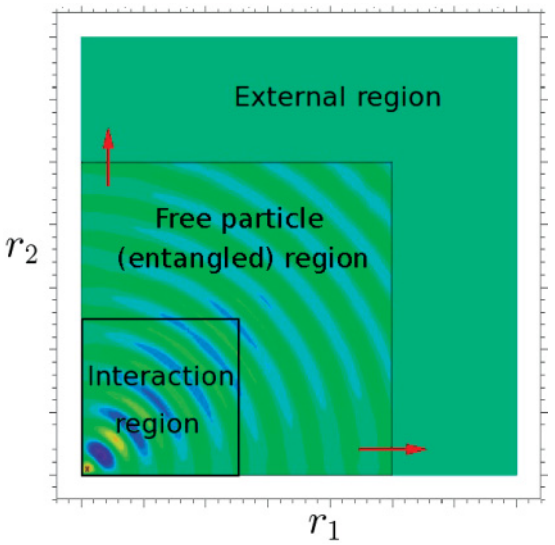

FIG. 3. (Color online) Different physical and computational domains.

The figures also show a schematic FEM griding, automatically generated by the FLEXPDE software (a denser mesh was used in all the presented calculations).

On the boundary $r_1 = 0$ we enforce the condition $\Psi^+_{sc} = 0$, while in $r_1 = r_2$ we consider $\partial_\alpha \Psi^+_{sc} = 0$ ($\Psi^+_{sc} = 0$), which is valid for the $S = 0$ ($S = 1$) symmetry. On the remaining contour we fix outgoing-flux conditions $\partial_{\mathbf{n}} \Psi^+_{sc} = (iK - \frac{5}{2\rho})\Psi^+_{sc}$, where $K = \sqrt{2E}$ and $\mathbf{n}$ is the direction normal to the contour. This last condition makes the main difference between the FEM calculations on the triangular (a) and the circular sector (b) domains. The case of domain (a) has connection with the CISF calculation, since the flux condition is considered in the radial coordinate direction instead of the hyperspherical one. It matches the hyperspherical case given by Eq. (12) only in the direction $\alpha = \pi/2$. Besides, in domain (b) the condition matches the form given by Eq. (12) in the whole arc. The sizes of both domains are characterized by the length r_c of the $r_1 = 0$ contour.

At this point we would like to emphasize the main difference between the FEM and the CISF calculations: in the first one, the functional space is finite (i.e., the external region in Fig. 3 is not included), while in the GSF expansion it can be finite or infinite depending on the region of integration of the overlap matrices.

IV. RESULTS

A. Analytically solvable model

We evaluate the scattering wave function corresponding to the energy $E = 0.881$ a.u. in Eq. (10) with both the Sturmian expansion and the FEM method in the two proposed domains. For simplicity, we choose a spherical well of radius $r_c = 50$ a.u. and 1 a.u. of depth to be the generating potential of the GSF basis. Any short-range potential would be adequate, although differences in the convergence properties may exist.

We present two choices of the energy of the two-body Sturmian equation: $E_1 = E_2 = E$ and $E_1 = E_2 = E/2$, where E is the total three-body system energy. Although the first choice does not completely remove the energy when the Galerkin

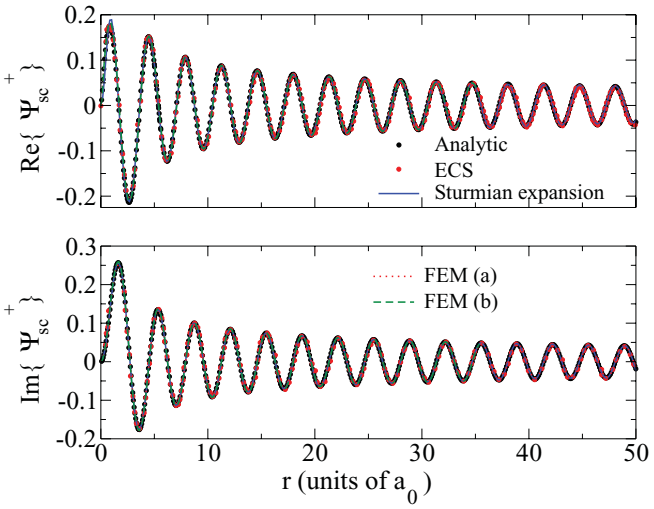

FIG. 4. (Color online) Expansion of the scattering wave function along the curve $r_1 = r_2$. Black line: Analytic result. Red circles: Exterior complex scaling result. Blue line: Sturmian expansion. Red and green lines: FEM solutions in domains (a) and (b), respectively.

method is applied, it gives better results than the second one, which does remove it. Other values were tested, giving worse results than the $E_1 = E_2 = E$ election.

Comparison between the CISF and FEM calculations in both domains can be seen in Fig. (4), where we plot the analytical and the ECS [18] results. The figure shows the real and imaginary parts of the scattered wave functions [solution of Eqs. (10), (11), and (12)] along the line $r_1 = r_2$ ($\alpha = \pi/4$), where the evaluations were done in a domain of $r_c = 50$ a.u. We see excellent convergence and coincidence between all methods in that domain.

We also study the convergence properties of the differential cross section as a function of the energy ε_1 of one of the outgoing particles, in other ($\alpha \neq \pi/4$) directions of the (ρ,α) plane. The differential cross section is related to the behavior of the wave function in the α coordinate at large values of ρ, since it is known that their energies are $\varepsilon_1 = \frac{1}{2}K^2\cos^2\alpha$ and $\varepsilon_2 = \frac{1}{2}K^2\sin^2\alpha$. Results are shown in Fig. (5), where we plot the progressive convergence of the cross section at $\rho = 30$ a.u., evaluated with the CISF expansion and the FEM calculation on domain (b), for different values of N_s (the number of two-particle GSFs) and finite elements, respectively, as a function of the dimensionless variable $\varepsilon = \varepsilon_1/E$. It is also indicated in the figures as the density (**d**) of basis elements per atomic unit of area.

GSFs' evaluations of densities $\mathbf{d}_{\mathrm{GSF}} = 0.186$ and $\mathbf{d}_{\mathrm{GSF}} = 0.51$, together with the FEM's evaluation with $\mathbf{d}_{\mathrm{FEM}} = 9.963$ cannot be clearly seen because they lie over the analytic result. Note the difference in the performance of both methods. We can compare the efficiency of the GSF basis over the finite elements by the coefficient $\mathbf{d}_{\mathrm{FEM}}/\mathbf{d}_{\mathrm{GSF}} = 53.5645$.

In order to show the effect of each contour, we compare the cross section results of both FEM calculations evaluated at $\rho = 20$ for different values of r_c ($r_c = 30$, 40, and 50 a.u.). Results are shown in Figs. 6(a) and 6(b).

The first phenomena to be noted is that the FEM calculations in the domain (a) show oscillations around the exact value. This implies that oscillations are related to the boundary condition imposed by the FEM method in the square geometry. Since the calculation is performed in a box (there is no solution for $r_i > r_c$, $i = 1,2$) which does not have the appropriate symmetry, oscillations can be interpreted as reflection or overtransmission, followed by interference phenomena, with the consequence of having unphysical oscillations of the results around the exact value of the single differential cross section (SDCS) as a function of the energy fraction ε. To impose *directly* the adequate flux condition in the straight contour, the α dependence of it along the $r_2 = r_c$ should be used. Some other methods which employ square-type domains, like the ECS or one of the CISF presented here, induce the correct flux *indirectly*. Anyway, results for the different values of r_c shown in Fig. 6(a) suggest that the oscillations present in the triangular domain decrease in amplitude as r_c increases. On the other hand, the calculation in domain (b) [shown in Fig. 6(b)] has a smooth convergence. This is because the flux is imposed in the correct direction and interference does not occur.

A similar reflexion (or overtransmission) effect can be seen as a result of the CISF calculation in the box [see Fig. 7(a)]. In this case the calculation is similar to the FEM

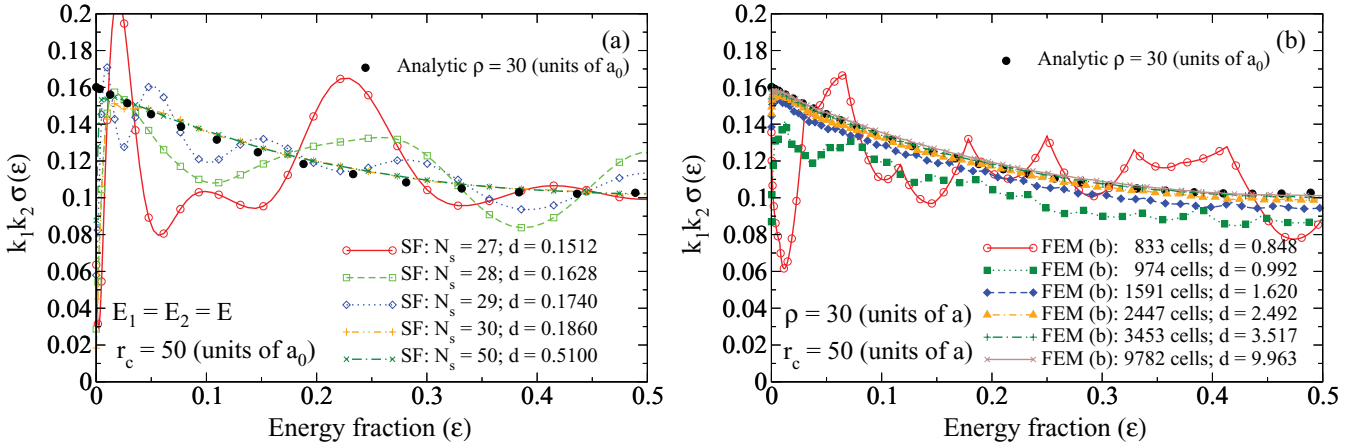

FIG. 5. (Color online) Convergence properties of the Sturmian function expansions (a) and FLEXPDE (b). In both graphs the curves are symmetrical with respect to the point $\varepsilon = 0.5$.

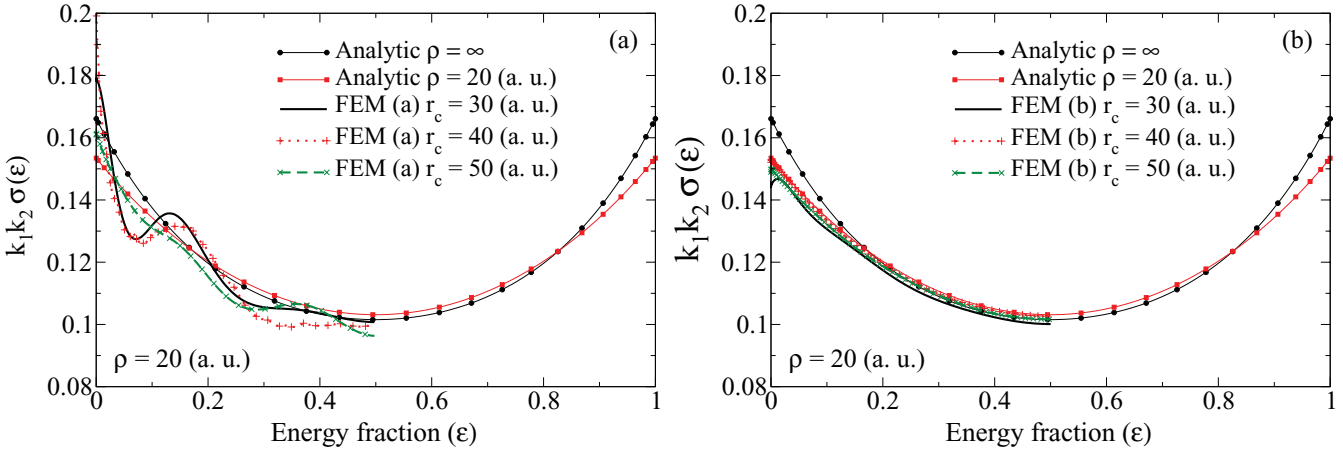

FIG. 6. (Color online) Convergence of the FEM solutions for domain (a) [panel (a)] and domain (b) [panel (b)].

one since it is assumed that no particle reaches the region $r_i > r_c$ $(i = 1,2)$. The oscillations are present for the basis parameters $E_1 = E_2 = E$ and $E_1 = E_2 = E/2$, but are more intense in the second case. The calculation with the parameters $E_1 = E_2 = E$ gives results similar to those with the FEM calculation in domain (a). The oscillations of the $E_1 = E_2 = E/2$ case decrease in magnitude when the scalar product and overlap matrices are defined in the whole space [see Fig. 7(b)]. The Sturmian expansion with the scalar product in the infinite domain and a Sturmian energy equal to the total three-body system energy [Fig. 7(b)] shows an excellent agreement with the FEM calculation in domain (b) and also with the exact result. This indicates that continuing the definition of the wave function in the entire spatial domain makes the quantum mechanical flux well represented in all directions.

Of course, a finite basis calculation has a finite spatial range of validity characterized by r_c, and the minimum number of GSFs needed to obtain convergence increases with r_c, even if the major part of the domain is a noninteracting region. This is because the hyperspherical wave is nonseparable in spherical coordinates [see Fig. 3]. In the region $r_c \leqslant r_i < \infty$ $(i = 1,2)$ the wave function is associated with the case in which one or two particles escape from the central potential with a fixed energy given by E_1 and E_2. This part of the wave function does not contain relevant information about the system's dynamics.

Results show that, although the "box" calculations with GSF and FEM methods do not give exactly the same results, they present similarities in their oscillations. From all the CISF calculations of Fig. 7 we clearly see that the optimal flux property of the basis is that associated with the total energy $E_1 = E_2 = E$ (we have also tested convergence for other energy-basis parameter values and have obtained worse results).

B. Temkin-Poet model for electron hydrogen ionization

Here we briefly demonstrate the application of both methodologies discussed above to solve the Temkin-Poet model of electron hydrogen ionization. First we study both the CISF and FEM calculations for this model with Coulomb interactions in small domains. Second, we analyze the CISF differential cross section compared to the exact result.

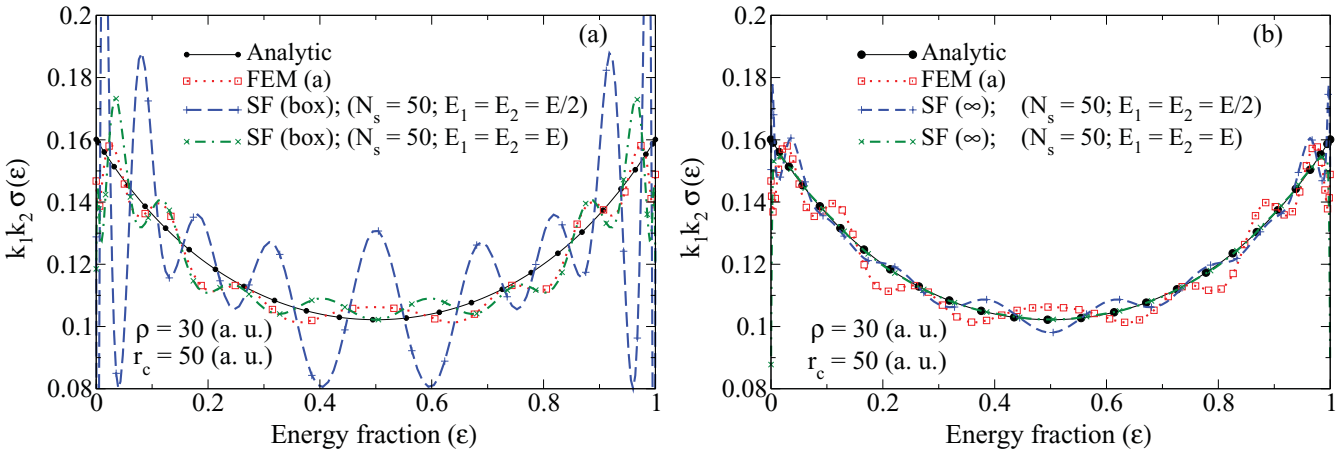

FIG. 7. (Color online) GSF expansion where the cases $E_1 = E_2 = E$ and $E_1 = E_2 = E/2$ [E_i $(i = 1,2)$ basis energy] are considered. In panel (a) the contribution of Eq. (19) is not taken into account (we denote the calculation as "box"), while in panel (b) it is considered (we denote the calculation as "∞").

The scattering wave function for this problem is the solution to the nonhomogeneous Schrödinger equation:

$$\left[-\frac{1}{2}\frac{\partial^2}{\partial r_1^2}-\frac{1}{2}\frac{\partial^2}{\partial r_1^2}-\frac{1}{r_1}-\frac{1}{r_2}+\frac{1}{r_>}-E\right]\Psi_{sc}^{+}(r_1,r_2)$$
$$=-\left[\left(\frac{1}{r_>}-\frac{1}{r_2}\right)\Psi_0(r_1,r_2)+(-1)^S(1\longleftrightarrow 2)\right], \qquad (21)$$

where $r_> = \mathrm{Max}[r_1,r_2]$ and $k_i = \sqrt{2[E-(-0.5)]}$ is the momentum of the particle which collides with the H atom in its ground state. The unperturbed initial state can be written as

$$\Psi_0(r_1,r_2) = -\frac{1}{\sqrt{8\pi k_i}}[(2e^{-r_1}r_1)\sin(k_i r_2)+(-1)^S(1\longleftrightarrow 2)].$$

Note that despite the presence of the Coulomb potentials, the nonhomogeneity in the right-hand side of Eq. (21) has a short-range character determined by the exponential in one of the coordinates and the $(r_>^{-1}-r_i^{-1})$ $(i=1,2)$ terms.

We use the GSF expansion and the FEM domain which gave results without oscillations for the analytically solvable model.

Figure 8 shows the real part of the scattering wave function for $S=0$ evaluated with the Sturmian expansion. The function presents the typical hyperspherical wave behavior superposed on the discrete elastic and excitation channels (peaks close to the axes).

The density plot of the FEM calculation showed in Fig. 9 exhibits the same properties. The grid superposed on the graphic is only schematic. A denser one was necessary to evaluate the wave function.

Agreement between both calculations can be seen from Fig. 10, where we plot the real and imaginary parts of the wave function along the $r_1 = r_2$ line.

C. Sturmian calculation of the SDCS

The convergence of the SDCSs for Coulomb interactions requires large numerical domains in the evaluation of the wave function, because of their long-range character. We employed the Sturmian function calculations, where we use the values $r_c = 130$ a.u. for the impact energies 40.817 and 54.4 eV and $r_c = 50$ a.u. for 150 eV. For the higher impact energy the wave function is much more oscillatory and there are necessarily more basis functions to represent the solution in a given numerical domain than for the lower energies. The calculation was done in all cases with $N_s = 175$ basis functions per coordinate, which correspond to the density $\mathbf{d}_{\mathrm{GSF}} = 0.9112$.

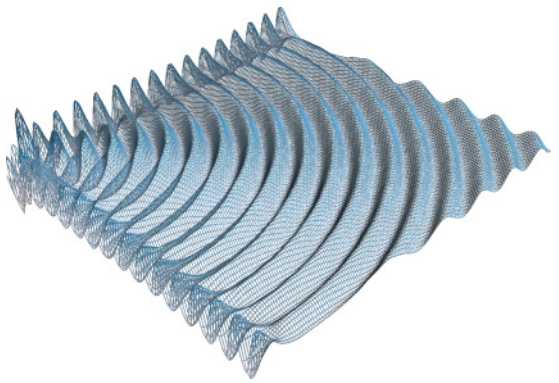

FIG. 8. (Color online) Schematic view of the real part of the scattering wave function evaluated with the Sturmian expansion.

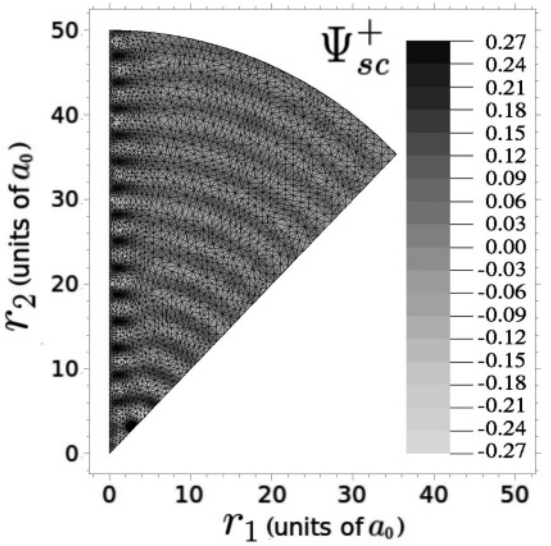

FIG. 9. Density plot of the FEM solution of Eq. (21). This figure also shows a schematic mesh (denser ones were used in the calculations), automatically generated with FLEXPDE.

Results of the SDCS evaluated with the CISF are shown in Fig. 11, where we compare them with the results of Jones and Stelbovics [9] with a variable-spacing finite-difference algorithm [10] and with the results of Baertschy *et al.* [19] and Bartlett and Stelbovics [37] with the exterior complex scaling method.

The technique used to extract the breakup cross sections is the flux formulas given by Peterkop [38] and the extrapolation procedure described by Rescigno and McCurdy [19,33]:

$$\frac{d\sigma}{d\varepsilon_1} = \frac{2}{K^2\sin\alpha\cos\alpha}\lim_{\rho\to\infty}\sigma_{\rho_0}(\alpha),$$

where σ_{ρ_0} is defined as

$$\sigma_{\rho_0}(\alpha) = \frac{4\pi}{k_0^2}\mathbf{F}(\boldsymbol{\rho}_0,\alpha)\cdot\rho_0,$$

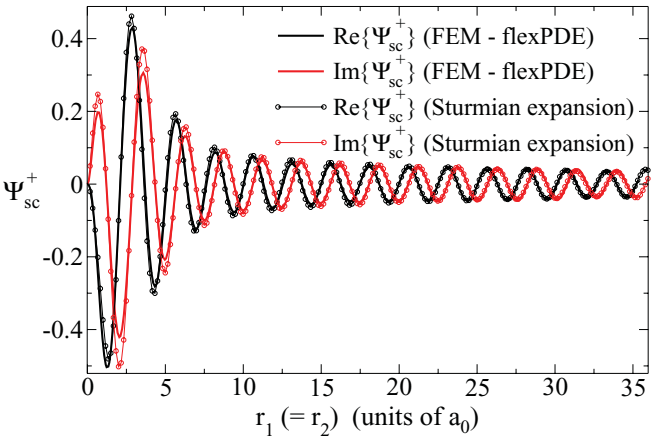

FIG. 10. (Color online) Comparison between the FEM and CISF calculations of Ψ_{sc}^{+} along the curve $r_1 = r_2$.

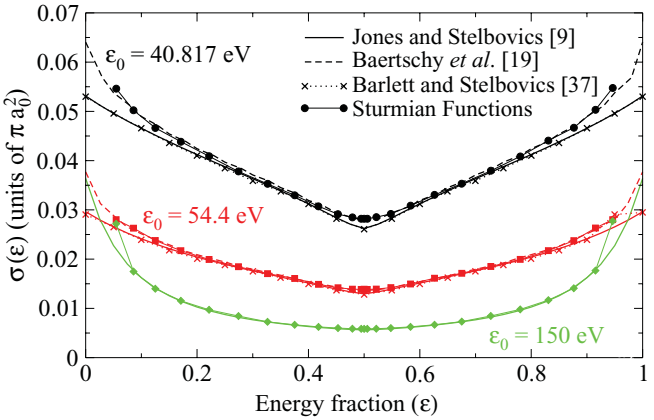

FIG. 11. (Color online) Comparison between single differential cross-section results of hydrogen ionization by electron impact, for incident electron energies equal to 40.817 eV (black, top curves), 54.4 eV (red, middle curves), and 150 eV (green, bottom curves).

where $\mathbf{F}$ is the quantum mechanical flux, $\mathbf{F} = (1/2i)(\Psi^*\nabla\Psi - \Psi\nabla\Psi^*)$, and $\rho_0 = (k_1/K, k_2/K)\rho_0$.

The numerical result can be estimated by extrapolating σ_{ρ_0} to an infinite ρ according to the law $\sigma_{\rho_0} = \sigma_{\rho_0}(\infty) + O(\rho^{-1})$. This formula is valid for the ionization region, and close to the points $\alpha = 0$ and $\alpha = \pi/2$ it can be polluted by elastic and excitation channels, given less accurate values. In Fig. 12 we show the behavior of the expression (22) for different values of ρ and the extrapolated result for 54.4 eV impact energy.

At $\alpha = \pi/4$ there is a discontinuity in the derivative of the SDCS with respect to α in the results of Jones and Stelbovics [9]. This characteristic peak can be reproduced by using integral formulas with final states which have a discontinuity at $\alpha = \pi/4$ [associated with the discontinuity of the potential $r_>^{-1}$ present in Eq. (21)]. These states consist of a plane wave for the faster electron and a Coulomb wave for the slower one, in order to take into account the screening of the central potential by the slower electron [37]. The smooth curvature given by the flux formulas at this point becomes more pronounced when r_c is increased.

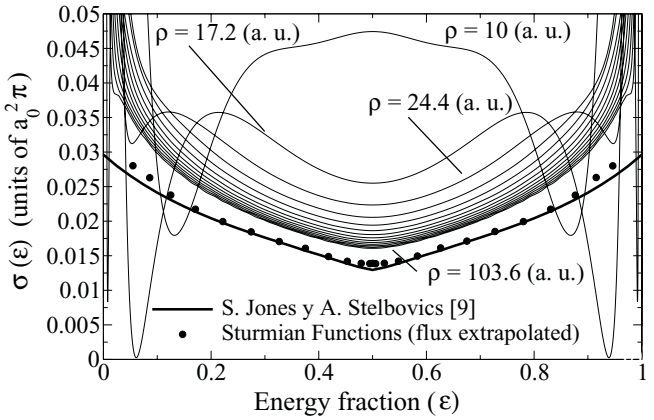

FIG. 12. Evaluation of the flux formula approximation of Eq. (22) from Ψ_{sc}^+ for an incident electron energy equal to 54.4 eV. We take 14 equally spaced (two wavelengths) values of ρ between 10 and 103.6 a.u. We also show the extrapolated result (circles), and the results of Jones and Stelbovics [9] (continuous line).

D. Comparison of the efficiency

The computational methods used in scattering problems reduce finally to a linear system of equations, whose size is related to the number of basis elements employed. This size is limited by the computational resources. To obtain convergence in a given computational domain, a minimum number, $n_{\min}$, of basis elements is required. Given the local qualities of the FEM basis, and the more sophisticated (physical) equation from which SFs are defined, it is obvious that for a fixed size of the domain $n_{\min}^{(\mathrm{GSF})} < n_{\min}^{(\mathrm{FEM})}$. However; the locality of the FEM basis makes the linear system sparse and not a full one as is the case when using CISF or other spectral methods. FEM software takes advantage of this and requires less computational resources: for a fixed memory resource the property $n_{\min}^{(\mathrm{GSF})} < n_{\min}^{(\mathrm{FEM})}$ is always possible. Another important difference between the CISF and FEM calculations is that the FLEXPDE [36] software uses iterative methods to minimize the error of the proposed solution and not (necessarily) to find the exact solution of the (large) linear system. On the other hand, with the GSF expansion we employ LU decomposition (i.e., the involved matrix is written as a product of a lower diagonal by a upper diagonal matrices) with partial pivoting performed by the ZGESV subroutine of LAPACK.

With these considerations in mind, the differences in the efficiency should be studied taking into account two important factors: (1) the maximum precision of a solution for a fixed computational resource, and (2) the time of the calculation. Such study was performed in a vibroimpact, time-dependent mechanic system by Ritto *et al.* [39], between the FEM basis and the proper orthogonal decomposition (POD) method (which is an optimized basis also called Karhunen-Loëve decomposition [40]). The conclusion was that the POD solution is more efficient. A similar study is necessary for the problems presented here and is a matter for future publication. However we can develop some conclusions from the results obtained in the previous section.

With an Intel(R) Pentium(R) 4 CPU 3.0-Hz processor computer with 512 MB RAM, 32 bits, we evaluated the curves of Fig. (5) and compared the running time until a converged result was obtained. In Fig. 5(a) we can find a converged result with the GSF for $N_s = 30$ (orange dash-dotted line). The time of the calculation of the basis strongly depends on the parameters involved in the Sturmian Eq. (1) and the numerical routine's parameters such as mesh density and other ones that ensure good convergence. For this problem (with 100 grid points per atomic radial unit), it was between 5 and 6 s (7 and 8 s for $N_s = 50$). The time to evaluate the matrix elements and solve the linear system was 54 s (177 for $N_s = 50$). On the other hand, the converged FEM result (brown dot-dashed line) with the denser grid took 5 min and 27 s (327 s).

We would like to point out one of the major convergence problems which we were able to overcome after several proofs. When trying to establish FEM calculations with very dense grids, sometimes a minimal-error solution is reached which does not correspond to the physical solution. For example, some solutions have small but important differences in the amplitudes for the real and imaginary parts of the wave function, although they give correctly the wavelength and the global shape. This usually happened for big domains (where the number of elements must be huge). We think

this is related to the fact that the real and imaginary parts of the wave function are coupled only in the contour and through the boundary condition, but not in the whole space by the differential equation itself. Thus, a small error in the region close to the boundary can be amplified in the inner regions. In order to avoid this problem, we have applied an empirical methodology to obtain the FEM solutions presented in this article, which consists of the following. First, a rough (low-density grid) calculation is performed. When the density of the grid is low, these differences in the amplitudes are not too big, but a noisy solution is obtained instead. Then, the solution with correct amplitude is taken as the initial condition of a new calculation, this time with a denser grid. In this way, the density can be progressively increased to obtain a very good solution. Of course, the time to obtain the final solution becomes very large, and each iteration takes more time than the one which precedes it. This procedure gave good results for domains from $r_c = 20$ to 80 a.u. When we tried to apply it to the Temkin-Poet model in a domain of 130 a.u., the time of each iteration became very large, the last iteration tested had a density of $d_{\mathrm{FEM}} = 16.2726$ (107 995 cells) and took about 3 h, giving an unsatisfactory result. On the other hand, the CISF calculation presented for the Temkin-Poet model in a domain given by $r_c = 130$ a.u. (with density $\mathbf{d}_{\mathrm{GSF}} = 0.91$) took about 2 h with a desktop computer.

In order to compare the efficiency of the Sturmian expansion with other theories, we can cite the work of Rescigno *et al.* [13], in which for the complete problem of ionization of atomic hydrogen by electron impact with the exterior complex scaling (ECS) method they reach full matrix equation system, associated with a density of $d_{\mathrm{ECS}} \simeq 14.8$. On the other hand, in a newer implementation of this methodology called propagating ECS (PECS) [12], which uses a discrete variable representation with different griding regions, a result in a square domain of $R_0 = 220$ a.u. divided in $\simeq$625 intervals was presented. The density of basis elements is then $d_{\mathrm{PECS}} \simeq 626^2/220^2 \simeq 8.1$. Finally, we can mention the time-dependent calculation of Pindzola and Robicheaux [41], which uses grid points characterized by $\Delta r = 0.2$ a.u. and domains of side $R_0 = 100$ a.u. to $R_0 = 500$ a.u. in steps of 100 a.u., to evaluate the solution of the time-dependent (TD) Schrödinger equation corresponding to the TP model of the e-H processes. The best result is that of $R_0 = 500$ a.u. In all cases the density of basis elements is $d_{\mathrm{TD}} = 25$.

V. CONCLUSIONS

We compared the Sturmian expansion methodology to solve three-body fragmentation processes reported in Ref. [24] with various FEM calculations.

We performed FEM calculations in triangle- and square-shape domains and found that they are adequate since they are able to describe the cross sections, although introducing spurious oscillations. These oscillations appear since the outgoing-wave condition in a rectangular boundary is not related with the true geometry of the problem. Oscillations are related to the fact that the boundary condition describes the flux through the boundary approximately. The FEM calculation in domain (b) consists of a direct way to model the ionization behavior given by Eq. (12), since it has the adequate hyperspherical symmetry which allows imposition of the outgoing-flux condition, without making assumptions on the dependence of the wave function in the hyperangle α.

Two Sturmian expansions have been used in this work: one in a box domain, and the other one in the whole radial domain. The first one introduces the spurious oscillations, similar to those present in the FEM calculation in the triangle and square domains. The CISF calculation defined in the infinite space gave excellent results, both for short-range interactions and also for Coulomb-type scattering problems. Convergence of the wave functions and cross sections was found for both the CISF and FEM calculations, giving coincidence with analytical and ECS results of the short-range model problem.

For the TP model of the e-H processes, the Sturmian expansion gave results in excellent agreement with those of Baertschy *et al.* [19] and also in good agreement with those of Jones and Stelbovics [9,10] with a variable-spacing finite-difference algorithm and with those of Bartlett and Stelbovics [37] with the ECS method. The discrepancies we found at the extremes of the energy sharing in comparison with the previous two references (the benchmark solutions) are associated with the fact that the flux formula includes the contribution of the excitation and elastic channels present on the total wave function. For increasing values of ρ ($\rightarrow \infty$), that region shrinks to a negligible width, making the flux formula well defined in the whole range. Those contributions are eliminated in alternative formulations for the scattering amplitude, presented in Refs. [37] and [9]. We have not implemented those methodologies in our approaches; this will be a matter for future work. It worth noting that we are obtaining, except at the borders, basically the same result as all the precedent theories even using smaller evaluation domains.

FLEXPDE software for FEM is also able to evaluate the TP scattering wave function. However, we do not obtain accurate values of the wave functions in big enough domains. This is because in big domains (necessary to evaluate SDCS when Coulomb interactions are present) the iterative algorithms which minimize the error of the solution are inaccurate. We have developed a preconditioning procedure based on several calculations with a progressive increase of the number of finite elements. The success of this methodology, together with the intermediate preconditioned results, confirms in some way our theory about the origin of the errors when a unique very dense grid evaluation (without preconditioning) is performed. We think that those errors are amplifications of small errors close to the boundary conditions, which is the only coupling between the real and imaginary parts of the scattering wave functions. The time of the evaluation of the wave function for big domains becomes too large to be used for practical purposes.

The two methods introduced here correspond to two ways to overcome the difficult task of describing the proper and unknown asymptotic condition from a boundary condition, in the evaluation of the scattering wave function of fragmentation problems. From Eq. (10) one can easily see that $\mathrm{Re}\{\Psi_{\mathrm{sc}}\}$ is the solution of a nonhomogeneous second-order differential equation, while $\mathrm{Im}\{\Psi_{\mathrm{sc}}\}$ is the solution of a homogeneous one, both with stationary-wave behavior. The amplitude of $\mathrm{Re}\{\Psi_{\mathrm{sc}}\}$ is coupled to that of $\mathrm{Im}\{\Psi_{\mathrm{sc}}\}$ through the boundary condition. If we tried to solve for both equations independently with real stationary-wave radial Sturmian functions (easily

obtained with the numerical methods that we employed here), the hyperspherical symmetry would not be necessary obtained. Instead, a basis in hyperspherical coordinates would be preferable [34]. With the outgoing-wave behavior basis introduced here, the correct symmetry is obtained. Although the Sturmians have the conditions imposed in the r_1 and r_2 directions, the hyperspherical behavior is well represented by the basis. It has to be taken into account that the hyperspherical behavior should be present in the whole asymptotic region, even if in that region the particles do not interact. It is associated with a highly correlated state, which is not separable in spherical coordinates but it is very simple in hyperspherical ones. The Sturmian expansion has to construct the solution in the domain proposed (square of side r_c), and the minimum number of basis elements increases with r_c. We can say that the basis has the asymptotic behavior corresponding to a (one of the many) solution of the asymptotic form of the Schrödinger Eq. (10), but it does not have the asymptotic behavior of the scattering solution. However, they are able to expand correctly the hyperspherical behavior. More research in that direction is needed in order to understand this point. Finally, we demonstrated one of the main advantages of the Sturmian expansion (aside from correctly constructing the hyperspherical wave); that is, CISF is a spectral method, which means that the computational resources are optimized. Furthermore, CISF can be easily extended to more than two-electron problems, which would not be the case for a hyperspherical basis calculation.

ACKNOWLEDGMENTS

This work has been supported by PGI (24/F049) of the Universidad Nacional del Sur, by ANPCyT (PICT08/0934) (Argentina), and by PIP 200901/552 CONICET (Argentina).

APPENDIX

1. Equations of motion in weak form

Let W_r and W_i be a real test (admissible) function of variables r_1 and r_2. Call $\psi_r(r_1,r_2) = \mathrm{Re}[\psi^+_{sc}(r_1,r_2)]$ and $\psi_i(r_1,r_2) = \mathrm{Im}[\psi^+_{sc}(r_1,r_2)]$. Multiplying the real part of the Schrödinger equation, Eq. (21), by W_r, and W_i by the imaginary one, and integrating over the two-dimensional domain S we get

$$\int_S \left(-\frac{1}{2}\nabla^2 - V - E\right)\psi_r W_r dS = \int_S g(r_1,r_2) W_r\, dS \quad \text{(A1)}$$

$$\int_S \left(-\frac{1}{2}\frac{\partial^2}{\partial r_1^2} - \frac{1}{2}\frac{\partial^2}{\partial r_2^2} - V - E\right)\psi_i W_i dS = 0, \quad \text{(A2)}$$

where $g(r_1,r)$ is given by the right-hand side of Eq. (21) and $V = \frac{1}{r_1} + \frac{1}{r_2} - \frac{1}{r_>}$. Since all well-behaved functions P and Q satisfy

$$\int_S (P\Delta\varphi + \nabla Q\cdot\nabla P)\, dS = \oint_{\partial S} P\,(\nabla Q\cdot\mathbf{n})\, dl, \quad \text{(A3)}$$

where ∂S is the boundary of domain S and $\mathbf{n} = [n_1,n_2]$ is the unitary vector normal to dl, then the second-order derivative terms can be written as

$$\int_S \nabla^2\psi\cdot W\, dS = \oint_{\partial S}\frac{\partial\psi}{\partial n} W dl - \int_S \nabla\psi\cdot\nabla W dS,$$

where $\frac{\partial\psi}{\partial n}$ means $[\frac{\partial\psi}{\partial r_1}n_1 + \frac{\partial\psi_r}{\partial r_2}n_2]$.

The line integral is divided in two parts, ∂S_1 and ∂S_2. Suppose that the value of the wave function ψ^+_{sc} is prescribed in a part of the boundary's ∂S_1 (essential boundary conditions), while flux is given in the other part ∂S_2. This means the following boundary conditions on ψ^+_{sc}:

$$\psi^+_{\mathrm{sc}} = f_1(r_1,r_2) \quad \text{on} \quad \partial S_1 \text{ (essential)}, \quad \text{(A4)}$$

$$\frac{\partial\psi^+_{\mathrm{sc}}}{\partial n} = f_2(r_1,r_2) \quad \text{on} \quad \partial S_2 \text{ (natural)}. \quad \text{(A5)}$$

In the case of essential boundary conditions, the solution ψ must satisfy Eq. (A4) on ∂S_1 but the test function W must satisfy the homogeneous essential boundary condition. In our case the essential conditions are imposed on the curves $r_i = 0$ $(i = 1,2)$, with $f_1(r_1,r_2) = 0$. Then, in the variational problem of Eqs. (A1) and (A2), the admissible test functions W are defined with the conditions $W = 0$ on ∂S_1 and

$$W(r_1,r_2) \in \mathrm{Ad}m_1 = \left\{W \middle| \int_S (\nabla W)^2\, \mathrm{d}S < \infty\right\}. \quad \text{(A6)}$$

Hence, the integral over ∂S_1 is zero. In the region ∂S_2 we impose a Robin-type [42] natural boundary condition, $f_2(r_1,r_2) = (iK - \frac{5}{2\rho})\psi^+_{\mathrm{sc}}(r_1,r_2)$, which couples the equations for ψ_r and ψ_i. In this region the admissible functions must only satisfy the condition given by Eq. (A6).

Finally, the system of equations (A1) and (A2) reads

$$\int\left[\frac{1}{2}\nabla\psi_r\cdot\nabla W_r - (V+E)\,\psi_r W_r\right]dS = \int g\cdot W_r dS + \int_{\partial S_2}\left(-\frac{5}{2\rho}\psi_r - K\psi_i\right)W_r dl, \quad \text{(A7)}$$

$$\int\left[\frac{1}{2}\nabla\psi_i\cdot\nabla W_i - (V+E)\,\psi_i W_i\right]dS = \int_{\partial S_2}\left(K\psi_r - \frac{5}{2\rho}\psi_i\right)W_i dl \quad \text{(A8)}$$

2. Galerkin method and discretization in finite elements

Let $\{\phi_{\mathbf{j}}\} \in \mathrm{Ad}m_1$ be a base of a subspace of a Hilbert space. ϕ_i are shape functions with the properties of W. Let the function $\psi^+_{\mathrm{sc}}(r_1,r_2)$ be expanded in a series of vectorial functions $\phi_i(r_1,r_2)$:

$$\psi_r(r_1,r_2) \simeq \sum_{i=1}^{N} c_i\phi_i(r_1,r_2), \quad \text{(A9)}$$

$$\psi_{\mathbf{i}}(r_1,r_2) \simeq \sum_{i=1}^{N} d_i\phi_i(r_1,r_2). \quad \text{(A10)}$$

Here c_i and d_i are the unknown expansion coefficients. Replacing Eqs. (A9) and (A10) in Eqs. (A7) and (A8)

we get

$$(\boldsymbol{K}+\boldsymbol{E}+\boldsymbol{N})\boldsymbol{c}+\boldsymbol{M}\boldsymbol{d}=\boldsymbol{g} \tag{A11}$$

and

$$(\boldsymbol{K}+\boldsymbol{E}+\boldsymbol{N})\,\boldsymbol{d}-\boldsymbol{M}\boldsymbol{c}=\boldsymbol{0}, \tag{A12}$$

where $[\boldsymbol{c}]_i = c_i$, $[\boldsymbol{d}]_i = d_i$, $\boldsymbol{g}$ is the vector defined by $g_j = \int g\phi_j dv$, and $\boldsymbol{K}$, $\boldsymbol{E}$, $\boldsymbol{N}$, and $\boldsymbol{M}$ are matrices defined by

$$K_{ij} = \frac{1}{2}\int \nabla\phi_i \cdot \nabla\phi_j dS, \tag{A13}$$

$$E_{ij} = -\int (V+E)\phi_i\phi_j dS, \tag{A14}$$

$$N_{i,j} = \frac{5}{2}\int_{\partial S_2} \frac{1}{\rho}\phi_i\phi_j dl, \tag{A15}$$

and

$$M_{i,j} = K\int_{\partial S_2} \phi_i\phi_j dl, \tag{A16}$$

respectively.

[1] M. R. H. Rudge and M. J. Seaton, Proc. R. Soc. London A **283**, 262 (1965).
[2] M. R. H. Rudge, Rev. Mod. Phys. **40**, 564 (1968).
[3] E. O. Alt and A. M. Mukhamedzhanov, Phys. Rev. A **47**, 2004 (1993).
[4] A. S. Kadyrov, A. M. Mukhamedzhanov, and A. T. Stelbovics, Phys. Rev. A **67**, 024702 (2003).
[5] A. S. Kadyrov, A. M. Mukhamedzhanov, A. T. Stelbovics, I. Bray, and F. Pirlepesov, Phys. Rev. A **68**, 022703 (2003).
[6] F. D. Colavecchia, G. Gasaneo, and C. R. Garibotti, Phys. Rev. A **57**, 1018 (1998).
[7] G. Gasaneo, F. D. Colavecchia, C. R. Garibotti, J. E. Miraglia, and P. Macri, Phys. Rev. A **55**, 2809 (1997).
[8] A. S. Kadyrov, A. M. Mukhamedzhanov, A. T. Stelbovics, and I. Bray, Phys. Rev. A **70**, 062703 (2004).
[9] S. Jones and A. T. Stelbovics, Phys. Rev. A **66**, 032717 (2002).
[10] S. Jones and A. T. Stelbovics, Phys. Rev. Lett. **84**, 1878 (2000).
[11] C. W. McCurdy and T. N. Rescigno, Phys. Rev. A **62**, 032712 (2000).
[12] P. L. Bartlett, J. Phys. B **39**, R379 (2006).
[13] T. N. Rescigno, M. Baertschy, W. A. Isaacs, and C. W. McCurdy, Science **286**, 2474 (1999).
[14] E. Foumouo, G. L. Kamta, G. Edah, and B. Piraux, Phys. Rev. A **74**, 063409 (2006).
[15] V. A. Knyr, S. A. Zaytsev, Y. V. Popov, and A. Lahmam Bennani, J. Phys.: Conf. Ser. **141**, 012008 (2008).
[16] D. A. Konovalov, I. Bray, and I. E. McCarthy, J. Phys. B **27**, L413 (1994).
[17] K. Bartschat and I. Bray, J. Phys. B **29**, L577 (1996).
[18] T. N. Rescigno, C. W. McCurdy, W. A. Isaacs, and M. Baertschy, Phys. Rev. A **60**, 3740 (1999).
[19] M. Baertschy, T. N. Rescigno, W. A. Isaacs, and C. W. McCurdy, Phys. Rev. A **60**, R13 (1999).
[20] J. M. Randazzo, PhD. thesis, Instituto Balseiro, Universidad Nacional de Cuyo, 2009.
[21] D. M. Mitnik, F. D. Colavecchia, G. Gasaneo, and J. M. Randazzo, Comput. Phys. Commun. **182**, 1145 (2011).
[22] J. M. Randazzo, L. U. Ancarani, G. Gasaneo, A. L. Frapiccini, and F. D. Colavecchia, Phys. Rev. A **81**, 042520 (2010).
[23] J. M. Randazzo, A. L. Frapiccini, F. D. Colavecchia, and G. Gasaneo, Phys. Rev. A **79**, 022507 (2009).
[24] A. L. Frapiccini, J. M. Randazzo, G. Gasaneo, and F. D. Colavecchia, J. Phys. B **43**, 101001 (2010).
[25] S. Weinberg, Phys. Rev. **131**, 440 (1963).
[26] S. Weinberg, Phys. Rev. **133**, B232 (1964).
[27] Tricomi Confluent Hypergeometric Function: Series Representations (formula 07.33.06.0008) [http://functions.wolfram.com/07.33.06.0008.01].
[28] G. Rawitscher, Phys. Rev. C **25**, 2196 (1982).
[29] G. Rawitscher, e-print arXiv:1102.2172.
[30] J. H. Macek and S. Y. Ovchinnikov, Phys. Rev. A **54**, 544 (1996).
[31] P. M. Morse and H. Feshbach, *Methods of Theoretical Physics* (McGraw-Hill, New York, 1953).
[32] R. G. Newton, *Scattering Theory of Waves and Particles* (Dover Publications, New York, 2002), 2nd ed.
[33] T. N. Rescigno and C. W. McCurdy, Phys. Rev. A **62**, 032706 (2000).
[34] G. Gasaneo, D. M. Mitnik, A. L. Frapiccini, F. D. Colavecchia, and J. M. Randazzo, J. Phys. Chem. A **113**, 14573 (2009).
[35] Lapack—linear algebra package [http://www.netlib.org/lapack/].
[36] FLEXPDE finite element model builder for partial differential equations, PDE Solutions Inc, 2009 [http://www.pdesolutions.com/index.html].
[37] P. L. Bartlett and A. T. Stelbovics, Phys. Rev. A **69**, 022703 (2004).
[38] R. Peterkop, *Theory of Ionization of Atoms by Electron Impact* (Colorado Associated University Press, Boulder, 1977).
[39] T. Ritto, F. Buezas, and R. Sampaio, J. Sound Vib. **330**, 1977 (2011).
[40] M. Loeve, *Probability Theory II*, *Graduate Texts in Mathematics* (Springer, New York, 1977).
[41] M. S. Pindzola and F. Robicheaux, Phys. Rev. A **55**, 4617 (1997).
[42] S. Alfonzetti, G. BorzÃ¸and N. Salerno, Int. J. Numer. Methods Eng. **42**, 601 (1998).